Journal of Sound and Vibration (1997) **203**(3), 363–372

STRONG NON-LINEAR DYNAMICS OF CUTTING PROCESSES

C.-C. HWANG AND R.-F. FUNG

Department of Mechanical Engineering, Chung Yuan University, Chung-Li, Taiwan 32023, *Republic of China*

AND

J.-S. LIN

Department of Mechanical Engineering, Lien Ho College of Technology and Commerce, Miao-Li, Taiwan 360, *Republic of China*

(*Received* 2 *January* 1996, *and in final form* 21 *June* 1996)

A strong non-linear dynamic model is developed to investigate the dynamic characteristics of cutting processes. First, the multiple scales method is applied to study the weak non-linear stability, and then the numerical method to solve the problems of strong non-linearity in cutting processes. The former shows that the subcritical bifurcation predicted by the weak non-linear theory is compatible with that predicted by the strong non-linear theory. The numerical study reveals that different cutting thicknesses result in qualitatively different behavior of the finite amplitude instability. Going from small cutting thicknesses to the large ones, the behavior of the finite amplitude instability can be divided into an unconditional stable region, a conditional stable region, a periodic region and a breakdown region.

1. INTRODUCTION

Due to the non-rigid structures of a cutting system, chatter will result in inaccuracy of cutting. Therefore, to understand the chatter in cutting processes is a very important subject, that has been studied for a long time. As far as linear theories of chatter are concerned, the stability boundary has been found by Tobias [1], Merritt [2], Kato [3] and Wu [4] to distinguish between the linear stable and unstable regions in the space of the cutting parameters. However, such a linear theory cannot explain the behavior of finite amplitude instability, because a theoretical explanation of this behavior must be based on the non-linearities in the cutting processes. Non-linear cutting force due to higher order chip thickness variation is considered to be the reason for the finite amplitude vibrator [5, 6], and the multiple regenerative effect which is caused by the separation of the vibrating tool from the workpiece plays an important role in non-linear dynamic cutting [6–9]. Tobias [1], Hanna [5] and Shi [6] found that the cutting systems exhibit subcritical bifurcations. That is, the cutting process is dynamically stable when the level of disturbance is low, but unstable when it becomes higher. In their studies, the non-linear cutting forces were assumed to be a function of chip thickness only. Later, Lin and Weng [10, 11] showed that adding the effects of variation of shear angle strongly affected the dynamic cutting forces and cutting stability, and they found supercritical bifurcations only.

Although non-linear stability in metal cutting has been developed for a long time, only the weak non-linear theory was applied to the study of dynamic cutting processes. If the

0022–460X/97/230363 + 10 $25.00/0/sv960923

cutting systems are far from critical conditions or if the amplitudes of the disturbances are large enough, the weak non-linear theory may break down. Therefore, in order to obtain more accurate results, the cutting systems need strong non-linear analysis. In this paper, a multiple scales method is applied to the study of the weak non-linear dynamics in cutting processes. Then the numerical results of the strong non-linear equation help us to check the correctness of the weak non-linear theory. Furthermore, the strong non-linear theory can construct the global cutting phenomenon and cover the weak non-linear theory in the local regions around the critical conditions.

In this paper, we will develop a theory of strongly non-linear dynamics of cutting processes in the two-dimensional case. We find that the subcritical bifurcation predicted by the weak non-linear theory is consistent with that predicted by the strong non-linear theory; and the strong non-linear analysis can also predict the complex behavior of the cutting system.

2. DYNAMIC CUTTING MODEL

In this section, we will propose a two-dimensional non-linear dynamic cutting model, as shown in Figure 1. It can be formulated mathematically as follows:

$$m\ddot{x}^* + c_x\dot{x}^* + k_x x^* = F_x^* - \bar{F}_x^*$$
$$= \frac{(f_0 + x_T^* - x^*)d^*\tau_s \sin(\beta - \alpha)}{\sin\phi\cos(\phi + \beta - \alpha)} - \frac{f_0 d^*\tau_s \sin(\beta - \alpha)}{\sin\bar{\phi}\cos(\bar{\phi} + \beta - \alpha)}, \quad (1)$$

$$m\ddot{y}^* + c_y\dot{y}^* + k_y y^* = F_y^* - \bar{F}_y^*$$
$$= \frac{(f_0 + x_T^* - x^*)d^*\tau_s \cos(\beta - \alpha)}{\sin\phi\cos(\phi + \beta - \alpha)} - \frac{f_0 d^*\tau_s \cos(\beta - \alpha)}{\sin\bar{\phi}\cos(\bar{\phi} + \beta - \alpha)}, \quad (2)$$

where $x_T^* = x^*(t - T)$, m is the equivalent mass of tool block, c_x is the damping factor in the x direction, c_y is the damping factor in the y direction, k_x is the stiffness constant of the machine structure, k_y is the stiffness constant of the machine structure, F_x^* is the dynamic cutting force in the x direction, F_y^* is the dynamic cutting force in the y direction, $\bar{F}_x^*$ is the steady cutting force in the x direction, $\bar{F}_y^*$ is the steady cutting force in the y direction, f_0 is the feed rate, d^* is the width of cutting, τ_s is the shear stress, α is the rake

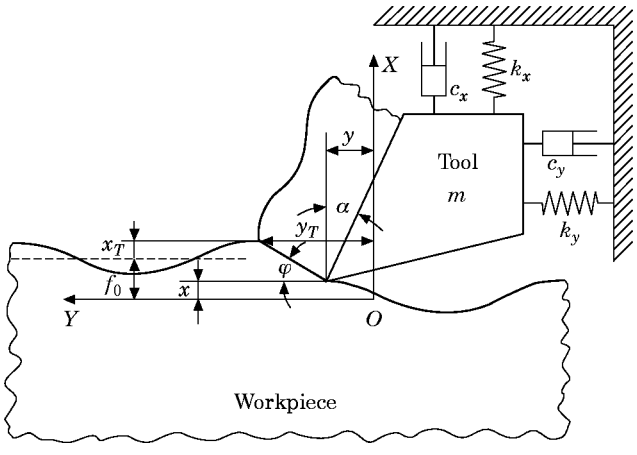

Figure 1. A model of chip formation in orthogonal cutting.

angle, β is the friction angle, ϕ is the shear angle, and $\bar{\phi}$ is the steady shear angle (note that a superscript asterisk represents a dimensional quantity).

Then a group of dimensionless quantities are introduced:

$$x_T^*/f_0 = x_T, \qquad x^*/f_0 = x, \qquad y^*/f_0 = y, \qquad t^*\omega_{n_x} = t,$$
$$\xi_x = c_x/(2\sqrt{k_x m}), \qquad d^*/f_0 = d, \qquad c_y/c_x = l_1, \qquad k_y/k_x = l_2, \tag{3}$$

where ω_n is the natural frequency in the x direction, and ξ_x is the damping ratio of the cutting tool system in the x direction.

After substituting the relations in (3) into equations (1) and (2), the dimensionless equation of motion becomes

$$\ddot{x} + 2\xi_x\dot{x} + x = F_x - \bar{F}_x$$
$$= d\frac{(1 + x_T - x)f_0\tau_s \sin(\beta - \alpha)}{k \sin\phi \cos(\phi + \beta - \alpha)} - d\frac{f_0\tau_s \sin(\beta - \alpha)}{k \sin\bar{\phi} \cos(\bar{\phi} + \beta - \alpha)}, \tag{4}$$

$$\ddot{y} + 2l_1\xi_x\dot{y} + l_2 y = F_y - \bar{F}_y$$
$$= d\frac{(1 + x_T - x)f_0\tau_s \cos(\beta - \alpha)}{k \sin\phi \cos(\phi + \beta - \alpha)} - d\frac{f_0\tau_s \cos(\beta - \alpha)}{k \sin\bar{\phi} \cos(\bar{\phi} + \beta - \alpha)}, \tag{5}$$

where $x_T - x + 1$ is the change of feed rate due to a regenerative effect.

Equations (4) and (5) are strong non-linear equations. The cutting parameters in equations (4) and (5) must be specified by experimental measurement, which is shown in Appendix A. In the following section, we will use the above equations to study the linear and non-linear dynamics of cutting processes.

3. LINEAR AND NON-LINEAR ANALYSIS

Since the stiffness and damping effects in the y direction are much larger than those in the x direction [12], for the sake of convenience and simplicity, we only consider the equation of motion in the x direction. Following Lin [10], we obtain the weakly non-linear equation of the shear angle variation and the regenerative effect:

$$\ddot{x} + 2\xi\dot{x} + x = Ad(x_T - x) - Bd(\dot{x}_T - \dot{x})[1 + (x_T - x)] + Cd(\dot{x}_T - \dot{x})^2[1 + (x_T - x)]$$
$$- Dd(\dot{x}_T - \dot{x})^3 + \tfrac{1}{3}BE^2d[(\dot{x}_T)^3 - \dot{x}^3]. \tag{6}$$

The parameters A, B, C, D and E are expressed as follows:

$$A = \bar{F}, \qquad B = -\left(\frac{\partial F}{\partial \dot{x}}\right)\Big|_{\bar{\phi}} E, \qquad C = \frac{1}{2!}\left(\frac{\partial^2 F}{\partial \dot{x}^2}\right)\Big|_{\bar{\phi}} E^2,$$

$$D = -\frac{1}{3!}\left(\frac{\partial^3 F}{\partial \dot{x}^3}\right)_{\bar{\phi}} E^3, \qquad E = \frac{f_0\omega_n}{V}. \tag{7}$$

By way of the linear stability analysis and by neglecting the non-linear portion of equation (6), the linearized equation becomes

$$\bar{x} + 2\xi\dot{x} + x = Ad(x_T - x) - Bd(\dot{x}_T - \dot{x}). \tag{8}$$

When we use normal mode analysis to solve equation (8), the solution is assumed as

$$x = \Gamma \exp(\mathrm{i}\lambda t) + c.c. \tag{9}$$

where Γ is an amplitude, $\lambda = \lambda_r + \mathrm{i}\lambda_i$ is a complex frequency, T is a rotating period of spindle, and $c.c.$ denotes the complex conjugate. Substituting equation (9) into equation (8), we can separate the real and imaginary parts of the characteristic equation as follows:

$$\text{Re: } -\lambda_r^2 + 1 = Ad(\cos \lambda_r T - 1) - Bd\lambda_r \sin \lambda_r T, \tag{10}$$

$$\text{Im: } 2\xi\lambda_r = -Ad \sin \lambda_r T - Bd\lambda_r(\cos \lambda_0 T - 1). \tag{11}$$

After choosing the chatter frequencies λ_r near the natural one and specifying the rotating periods T, the critical cutting thickness d_c can be found from equations (10) and (11). That is, the linear stability (instability) condition of steady cutting is $d < d_c (> d_c)$.

The linear stability analysis can only predict the linear behavior of the cutting processes. However, the finite amplitudes of the chatter that is caused by the non-linear cutting forces cannot be developed by linear stability theory. Therefore, in weak non-linear stability analysis, we used the perturbation method of multiple scales:

$$x(t_0, t_1, t_2) = \varepsilon x_1 + \varepsilon^2 x_2 + \varepsilon^3 x_3 + \cdots,$$

$$x_T(t_0, t_1, t_2) = \varepsilon x_{T1} + \varepsilon^2 x_{T2} + \varepsilon^3 x_{T3} + \cdots,$$

$$\frac{\mathrm{d}}{\mathrm{d}t} = \frac{\partial}{\partial t_0} + \varepsilon \frac{\partial}{\partial t_1} + \varepsilon \frac{\partial}{\partial t_2} + \cdots,$$

$$\frac{\mathrm{d}^2}{\mathrm{d}t^2} = \frac{\partial^2}{\partial t_0^2} + 2\varepsilon \frac{\partial^2}{\partial t_0\, \partial t_1} + \varepsilon^2 \left(\frac{2\partial^2}{\partial t_0\, \partial t_2} + \frac{\partial^2}{\partial t_1^2} \right) + \cdots. \tag{12}$$

Since the cutting thickness is an important parameter that strongly affects the dynamic stability, it can be taken as a perturbed quantity about the critical conditions. This can be expressed as

$$d = d_c + \varepsilon^2 \mu, \tag{13}$$

where d_c is the critical cutting thickness, $\varepsilon^2\mu$ is a small perturbed quantity, and $\mu = \text{sign}\,(d - d_c)$. Then, substituting equations (12) and (13) into equation (6) and solving equation (6) order by order, we can obtain the final form of Γ as follows:

$$\frac{\partial \Gamma}{\partial t_2} - \frac{\mu}{d_c}(X - \mathrm{i}Y)\Gamma - (L + \mathrm{i}M)d_c|\Gamma|^2\Gamma = 0, \tag{14}$$

where X, Y, L and M are shown in Appendix B.

The Landau type equation (14) can predict the weak non-linear dynamics near the regions of linear critical states. Weak non-linear stability analysis is carried out to study whether the finite disturbances in the linear stable region will cause instability (subcritical bifurcation) and whether the subsequent non-linear evolution of the disturbances in the linear unstable region will develop into another equilibrium with finite amplitude (supercritical bifurcation). Here the conditions of the subcritical (supercritical) bifurcations are $\mu = -1$ and $L > 0$ ($\mu = 1$ and $L < 0$), and the corresponding subcritical threshold (or supercritical finite) amplitude is equal to $\{[(d_c - d)X]/Ld_c^2\}^{1/2}$. According to our numerical evaluation, the cutting system only exhibits subcritical bifurcation ($L > 0$), which is the same as was found in Hanna's [5] and Shi's [6] research.

In addition, when the cutting system is far from the critical conditions or when the amplitudes of the disturbances are large enough, the weak non-linear theory may break down. For this reason, the only way to obtain more accurate evaluation is to use the full non-linear equation to study the strong non-linear dynamics of the cutting system. Due to the existence of the complicated non-linear term in dynamic equation (4), the numerical

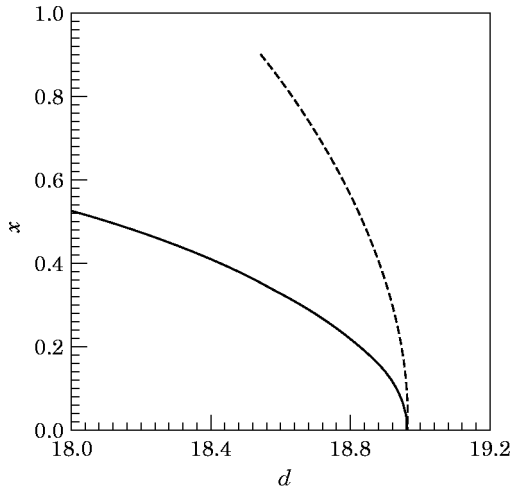

Figure 2. The local subcritical bifurcation diagram: $V = 150$ m/min, $f_0 = 0{\cdot}101$ mm, $T = 33{\cdot}2$. ——, Weak non-linear threshold amplitude; ----, strong non-linear threshold amplitude.

method introduced by Jemielniak and Widota [13], which is based on the determination of displacements, velocities and accelerations of the system in successive small periods, is applied to solve this equation with small initial disturbed conditions. When the multiple regenerative effect is considered, the position of the top surface of the chip to be removed is as follows: For $x_T - x + 1 > 0$, $x_T = x$, and for $x_T - x + 1 \leqslant 0$, $x_T = x_T + 1$.

4. RESULTS AND DISCUSSION

Here the characteristics of cutting stability under different feed rates, cutting velocities and cutting thicknesses are displayed and discussed first. Because the weak non-linear theory shows that only the subcritical bifurcation is possible, the linear stable region can be divided into two parts: one is the unconditional stable region and the other is the conditional stable region. In the unconditional stable region, the systems remain stable, although initial disturbances are finitely large. However, in the conditional stable region, the finite amplitude chatters will occur when initial disturbances exceed the threshold amplitude. The local subcritical bifurcation diagram predicted by the weak and strong non-linear theories is displayed in Figure 2. It shows that the subcritical bifurcation predicted by the weak non-linear theory is qualitatively consistent with that predicted by the strong non-linear theory, while the threshold amplitude of the strong non-linear theory is quantitatively larger than that of the weak non-linear one. In addition, the numerical results of the strong non-linear equations show that, in the conditional stable and linear unstable regions, the unstable disturbances will evolve into periodic states with finite amplitudes. However, if the system in the linear unstable regions is far from the linear critical condition and beyond another critical condition, any disturbance will grow to become infinite, and the cutting processes will break down. Here, in Figure 3 is shown the global bifurcation diagram predicted by the strong non-linear theory. The dashed line represents the initial threshold amplitude, and the solid line indicates the mean value of the final amplitude of periodic states. The periodic states calculated by way of the numerical method are always multiple ones. Since the variations of the amplitude, compared with their mean values, are very small, the multiple periodic states are not shown in Figure 3.

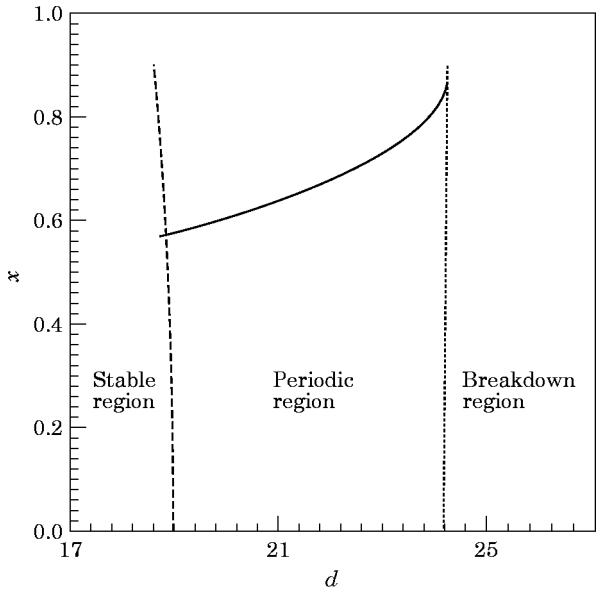

Figure 3. The global bifurcation diagram: $V = 150$ m/min, $f_0 = 0{\cdot}101$ mm, $T = 33{\cdot}2$. ——, Final amplitude of periodic states; ----, initial threshold amplitude.

From a global point of view, there are four types of dynamic behavior in cutting processes. They are steady unconditional stable states, steady conditional stable states, periodic states and breakdown states. The global stability basin in the T–d plane is shown in Figure 4. Generally speaking, for the fine cut (small cutting width), the operation conditions must be set in the unconditional stable region, while for rough cutting (large cutting width), they may be set in the periodic regions. With regard to the breakdown

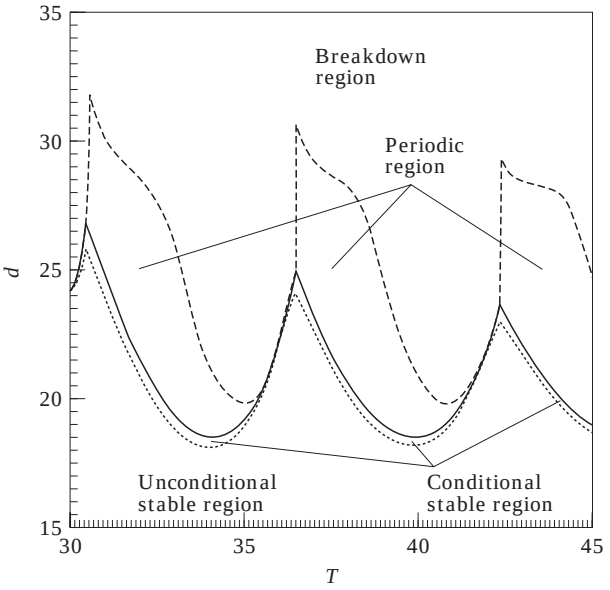

Figure 4. The cutting stability chart in the T–d plane. ——, Linear neutral stable line; · · · ·, the lower limit line of the periodic region; - - -, the upper limit line of the periodic region.

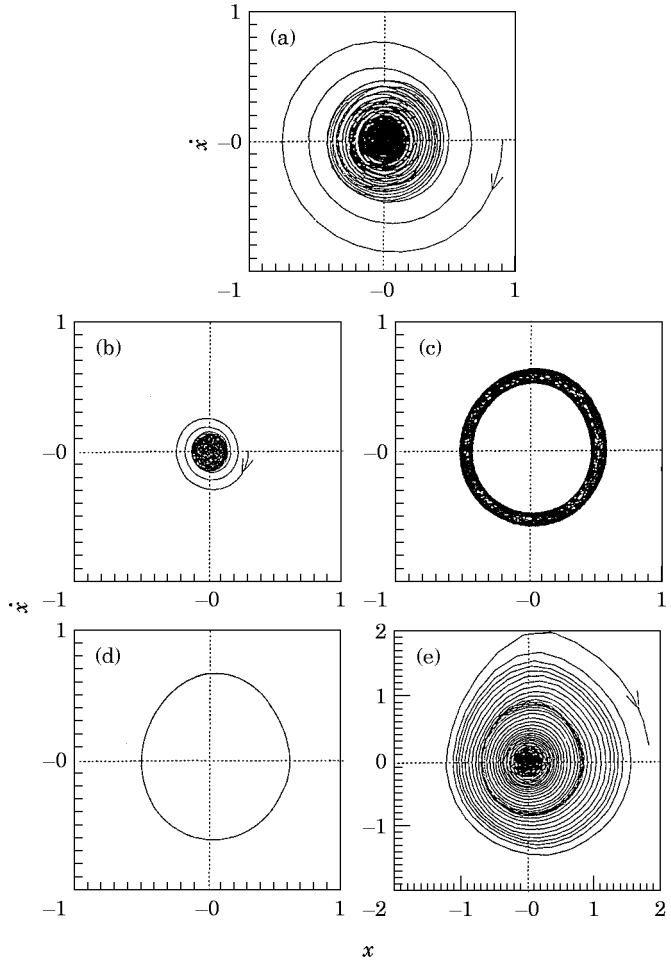

Figure 5. The phase planes of different types of motion: $V = 150$ m/min, $f_0 = 0{\cdot}101$ mm, $T = 37$, $\dot{x}(0) = y(0) = \dot{y}(0)$. (a) $d = 22$, $x(0) = 0{\cdot}9$; (b) $d = 22{\cdot}7$, $x(0) = 0{\cdot}3$; (c) $d = 22{\cdot}7$, $x(0) = 0{\cdot}9$; (d) $d = 26$, $x(0) = 0{\cdot}3$; (e) $d = 31$, $x(0) = 0{\cdot}01$.

region, no other operational condition can be set. On the other hand, in Figure 5 are shown the phase planes of the four types of motion mentioned above. First, an example of an unconditional stable state is shown in Figure 5(a). It is found that although the initial disturbance is as high as 0·9, the trajectory in the phase plane is convergent to zero. In addition, examples of the conditional stable region are shown in Figures 5(b) and 5(c). In Figure 5(b), we find that the trajectory of the phase portrait is convergent to zero when disturbances are small, but in Figure 5(c) it is shown that the path of the solution can develop into another limiting cycle when the initial disturbances are large. As shown in Figure 5(d), the periodic states will occur when the cutting thickness is larger than the linear critical cutting thickness. Furthermore, when the cutting thickness is larger than a non-linear critical one, the solution will then diverge to infinity even if the initial disturbances are very small, as shown in Figure 5(e).

Finally, the power spectra of the periodic states predicted by the numerical method and measured by the experimental method are shown in Figure 6, which represents the single and multiple periodic solutions. It is found that the principal spectrum densities of both

numerical and experimental methods are located near the natural frequency. The experimental data perhaps contain some noise, so there are random spectral distributions in all modes in Figures 6(a, ii) and 6(b, ii).

5. CONCLUSIONS

In this paper, we have developed a theory to predict the strongly non-linear dynamics in cutting processes. The perturbation method, together with multiple scales, is adopted to study the weak non-linear stability, and the numerical method is used to solve the full non-linear system of the cutting process.

It has been shown that the subcritical bifurcation predicted by the weak non-linear theory is consistent with that predicted by the strong non-linear theory. This subcritical bifurcation also constitutes Hanna's [5] and Shi's [6] experimental results. In addition the complex behavior of the cutting system can be found through the strong non-linear analysis. We have found that the cutting parameter space can be divided into four parts; i.e., the unconditional stable region, the conditional stable region, the periodic region, and the breakdown region. The rough cut cannot be set in the breakdown region, where the cutting operation is not available.

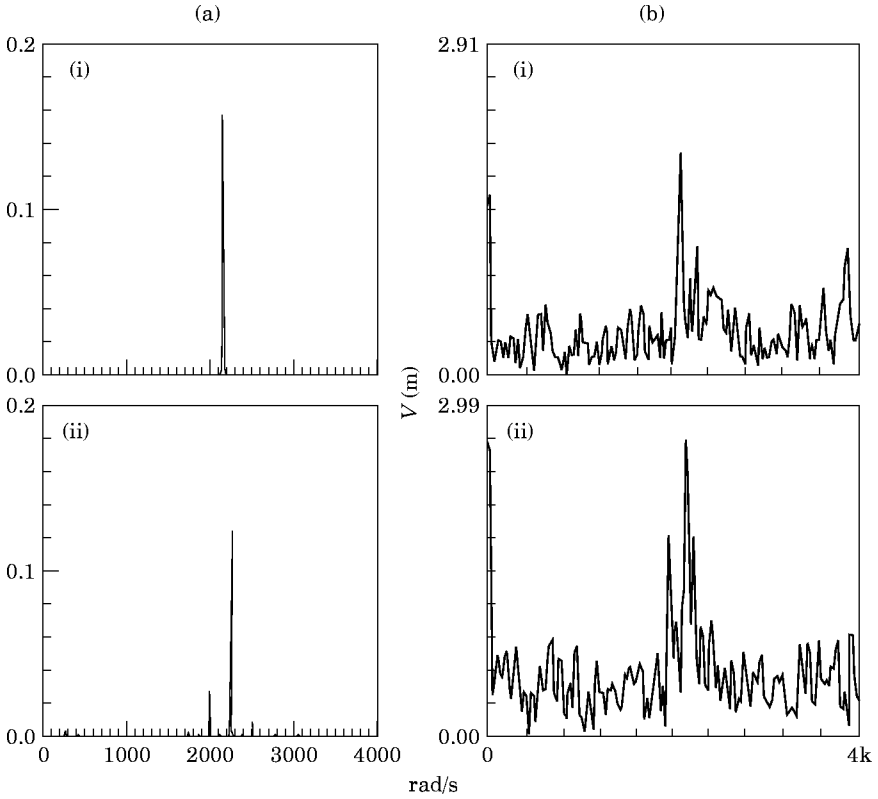

Figure 6. A comparison of the power spectral densities between the experimental and numerical results. (a) (i) = 150 m/min, $f_0 = 0{\cdot}101$ mm, $d = 29{\cdot}70$, $T = 39$; (ii) $V = 150$ m/min, $f_0 = 0{\cdot}101$ mm, $d = 23{\cdot}76$, $T = 37$. (b) Hanning spectra in the X direction.

ACKNOWLEDGMENT

The authors acknowledge with appreciation the financial support (Grant No. NSC 85-2212-3-239-001) provided by the National Science Council of the Republic of China.

REFERENCES

1. S. A. Tobias and W. Fishnick 1958 *Transactions of the American Society of Mechanical Engineers* **80**, 1079–1086. The chatter of lathe tools under orthogonal cutting conditions.
2. H. E. Merritt 1965 *Transactions of the American Society of Mechanical Engineers*, *Journal of Engineering for Industry* **87**, 447–454. Theory of self-excited machine tool chatter, condition to machine tool chatter Research-1.
3. S. Kato and E. Marui 1974 *Transactions of the American Society of Mechanical Engineers*, *Journal of Engineering for Industry* **96**, 179–186. On the cause of regenerative chatter due to workpiece deflection.
4. D. W. Wu and C. R. Li 1985 *Transactions of the American Society of Mechanical Engineers*, *Journal of Engineering for Industry* **107**, 107–188. An analytical model of cutting dynamics.
5. N. H. Hanna and S. A. Tobias 1974 *Transactions of the American Society of Mechanical Engineers*, *Journal of Engineering for Industry* **96**(1), 247–255. A theory of non-linear regenerative chatter.
6. H. M. Shi and S. A. Tobias 1984 *International Journal of Machine Tool Design and Research* **24**, 45–69. Theory of finite amplitude machine tool instability.
7. J. Tlusty and F. Ismail 1981 *Annals of the CIRP* **30**, 299–304. Basic non-linearity in machining chatter.
8. Y. Kondo, O. Kawano and H. Sato 1981 *Transactions of the American Society of Mechanical Engineers*, *Journal of Engineering for Industry* **103**, 324–329. Behavior of self-excited chatter due to multiple regenerative effect.
9. T. Kaneko, T. Sato, Y. Tani and M. O. Hori 1984 *Transactions of the American Society of Mechanical Engineers*, *Journal of Engineering for Industry* **103**, 222–228. Self-excited chatter and its marks in turning.
10. J. S. Lin and C. I. Weng 1990 *International Journal of Machine Tools and Manufacture* **30**, 53–64. A non-linear dynamic model of cutting.
11. J. S. Lin and C. I. Weng 1991 *International Journal Mechanical Sciences* **23**, 645–657. Non-linear dynamics of cutting process.
12. N. H. Cook 1959 *Transactions of the American Society of Mechanical Engineering*, *Journal of Engineering for Industry* **81**, 183–186. Self-excited vibration in metal cutting.
13. K. Jemielniak and A. Widota 1989 *International Journal of Machine Tools and Manufacture* **29**, 239–247. Numerical simulation of non-linear chatter in turning.
14. N. Saravanja-Fabris and A. F. D'Sonza 1974 *Transactions of the American Society of Mechanical Engineers*, *Journal of Engineering for Industry* **96**, 670–675. Non-linear stability analysis of chatter in metal cutting.

APPENDIX A: EXPERIMENTAL MEASUREMENTS

The main purpose of this experiment is to find τ_s in terms of the cutting velocity, the feed rate, and the spectrum of chatter in dynamic cutting.

First, the model testing analysis leads to the natural frequency, the damping ratio and the spring constant. They are, respectively,

$$\omega_{n_x} = 2030 \text{ rad/s}, \qquad \xi_x = 0{\cdot}087, \qquad k_x = 25\,000 \text{ Nt/mm}; \tag{A1a}$$

$$\omega_{n_y} = 3760 \text{ rad/s}, \qquad \xi_y = 0{\cdot}041, \qquad k_y = 85\,700 \text{ Nt/mm}. \tag{A1b}$$

In this experiment, carbide-insert tools are selected, with side rake angle $= 5^\circ$, side cutting angle $= 0^\circ$ and side clearance angle 6°, and the workpieces are of S45C.

The conditions of cutting test are as follows: feed rate, 0·101, 0·133, 0·177 mm/rev; cutting width, 2, 2·5, 3, 3·5, 4, 4·5 mm; cutting speed, 150, 200, 250, 300 m/min.

The cutting forces are found by means of a dynamometer, and the steady shear angle can be obtained through the geometric relationship of the cutting system. Combining the shear angle (ϕ), the side rate angle (α) and the friction angle (β), we have the following results [2, 14]:

$$K = 2\phi + \beta - \alpha = 79{\cdot}74^\circ \pm 3{\cdot}07^\circ. \tag{A2}$$

The curve fitting method is then applied to find the relation of τ_s in terms of the cutting velocity and the feed rate, and this equation can be expressed as follows:

$$\tau_s = \{1{\cdot}1748 \times 10^{-3}[V(\text{min/m})]^2 - 7{\cdot}1133 \times 10^{-1}[V(\text{min/mm})] - 9{\cdot}1701 \times 10^3[f_0/\text{mm}]^2 + 1{\cdot}8638 \times 10^3[f_0/\text{mm}] + 387{\cdot}25\}(\text{Nt/mm}^2). \tag{A3}$$

APPENDIX B

$$X = [(A_I C_I - B_I D_I)]/(C_I^2 + D_I^2), \qquad Y = [(A_I D_I + B_i C_I)]/(C_I^2 + D_I^2),$$
$$L = [(-Be_{II} + C\lambda_r^2 h_{II} + 3D\lambda_r^3 k_I)C_I + (-Bf_{II} + C\lambda_r^2 k_{II} - 3D\lambda_r^3 h_I)D_I]/(C_I^2 + D_I^2),$$
$$M = [(-Bf_{II} + C\lambda_r^2 k_{II} - 3D\lambda_r^3 h_I)C_I - (-Be_{II} + C\lambda_r^2 h_{II} + 3D\lambda_r^3 k_I)D_I]/(C_I^2 + D_I^2),$$
$$A_I = Ad_c(\cos\lambda_r T - 1) - Bd_c\lambda_r \sin\lambda_r T, \qquad B_I = Ad_c \sin\lambda_r T + \lambda_r Bd_c(\cos\lambda_r T - 1),$$
$$C_I = 2\xi + Bd_c(\cos\lambda_r T - 1), \qquad D_I = 2\lambda_r - Bd_c \sin\lambda_r T,$$
$$U = (a_I c_I + b_I d_I)/(c_I^2 + d_I^2), \qquad V = (b_I c_I - a_I d_I)/(c_I^2 + d_I^2),$$
$$a_I = -\{2Bd_c(\cos\lambda_r T - 1)\sin\lambda_r T + Cd_c[(\cos\lambda_r T - 1)^2 - \sin^2\lambda_r T]\lambda_r^2\},$$
$$b_I = Bd_c[\sin^2\lambda_r T - (\cos\lambda_r T - 1)^2]\lambda_r + 2Cd_c\lambda_r^2(\cos\lambda_r T - 1)\sin\lambda_r T,$$
$$c_I = -4\lambda_r^2 + 1 - Ad_c(\cos 2\lambda_r T - 1) + 2Bd_c\lambda_r \sin 2\lambda_r T,$$
$$d_I = 4\xi\lambda_r + Ad_c \sin 2\lambda_r T + 2Bd_c\lambda_r(\cos 2\lambda_r T - 1),$$
$$e_I = (\cos 2\lambda_r T - 1)(\cos\lambda_r T - 1) + (\sin 2\lambda_r T)\sin\lambda_r T,$$
$$f_I = (\cos 2\lambda_r T - 1)\sin\lambda_r T - (\cos\lambda_r T - 1)\sin 2\lambda_r T,$$
$$h_I = [(\cos\lambda_r T - 1)^2 - \sin^2\lambda_r T](\cos\lambda_r T - 1) + 2(\cos\lambda_r T - 1)\sin^2\lambda_r T,$$
$$k_I = [(\cos\lambda_r T - 1)^2 - \sin^2\lambda_r T]\sin\lambda_r T - 2(\cos\lambda_r T - 1)^2 \sin\lambda_r T,$$
$$e_{II} = -[(Uf_I + Ve_I)\lambda_r + E\lambda_r^3 \sin\lambda_r T], \qquad f_{II} = (Ue_I - Vf_I)\lambda_r - E(\cos\lambda_r T - 1)\lambda_r^3,$$
$$h_{II} = h_I + 4(Ue_I - Vf_I), \qquad k_{II} = k_I + 4(Uf_I + Ve_I).$$